MP2 and DFT Calculations of the Interaction Energies Between Boronated Aromatic Molecules and Small DNA Models: Applications to Cancer Therapy

I give permission for public access to my Honors paper and for any copying or digitization to be done at the discretion of the College Archivist and/or the College Librarian.

Signed_____

Kelly Allison

Date_____

MP2 and DFT Calculations of the Interaction Energies Between Boronated Aromatic Molecules and Small DNA Models: Applications to Cancer Therapy

Written at Rhodes College

Kelly Elizabeth Allison

Department of Chemistry
Rhodes College
Memphis, Tennessee

2012

Submitted in partial fulfillment of the requirements for the
Bachelor of Science degree with Honors in Chemistry

This Honors paper by Kelly Allison has been read

and approved for Honors in Chemistry.

Dr. Mauricio Cafiero
Project Advisor

_____

Dr. Larryn Peterson
Second Reader

_____

Dr. Erin Bodine
Extra-Departmental Reader

_____

Dr. Darlene Loprete
Department Chair

_____

CONTENTS

TABLES AND FIGURES

ABSTRACT

MP2 and DFT Calculations of the Interaction Energies Between Boronated Aromatic Molecules and Small DNA Models: Applications to Cancer Therapy

by

Kelly Elizabeth Allison

Boronated molecules are increasingly used in pharmacological applications, including cancer therapy. In boron-neutron capture therapy, boronated molecules localized in tumor cells are bombarded with slow neutrons in order to induce cell death. This work examines possible localization of boronated molecules in DNA by examining differences in interaction energies between boronated and non-boronated ligands with nucleic acid models. We have created complexes of boronated and non-boronated aromatic ligands with different nucleic acid sequences and optimized their structures. Counterpoise-corrected interaction energies for these single- and double-stranded complexes have been calculated using MP2, CCSD, and various DFT functionals with the 6-31+G* and 6-311+G* basis sets. Results show consistent differences in binding between boronated molecules and non-boronated molecules to nucleic acids within single-stranded DNA complexes. ONIOM(MP2:AM1) interaction energy calculations for boronated and non-boronated ligands within double-stranded DNA complexes largely agree with the single-stranded results. Double-stranded complexes were also modeled with and without charges on the phosphate groups and produced similar results. Interactions energies of a model hybrid intercalant possessing a dipole indicate improved interactions with charged, double-stranded complexes. The use of boron in intercalating drug design shows promise in enhancing the interaction strength and selectivity of DNA-targeted drugs.

1. Introduction

1.1 Pharmaceutical Potential of Boron

The demand for increasingly efficient drug design has been a point of focus in the field of pharmacological research in recent years. In the past, drug discovery was characterized by a labor-intensive system of screening thousands of compounds against hundreds of targets to identify candidates presenting a particular pharmacological activity.[i] Rational drug design, which takes advantage of the molecular recognition of drugs with specific targets and binding sites, is of particular interest because it is more efficient than screening. Specifically, it is valuable to understand the thermodynamics of drug-DNA interactions when designing selective DNA-binding drugs that can be used in different chemotherapeutic and anticancer treatments.

A variety of boronated molecules and systems have shown particular pharmaceutical potential due to observed anti-hyperlipidemic, anti-neoplastic, anti-inflammatory, anti-osteoporotic, and anti-obesity activity.[ii] As of March 2011, only one boron-containing prescription drug called Valcade® is on the market and acts as a treatment for multiple myeloma.[iii] Because of the extensive pharmaceutical potential of boronated compounds, a demand exists for the compilation of structural, kinetic, and thermodynamic data describing the interactions of these compounds in order to guide rational drug design and optimize boron's therapeutic potential.

The pharmaceutical potential of boron stems from its various structural and electronic properties that differentiate it from carbon, which is located immediately right of boron on the periodic table. First of all, while, like carbon, it is able to form small compounds of an appropriate size for targeting various biological binding sites, boron's

hydrides form cage or cluster-like structures with more geometric variability than the rigid chains and rings formed by carbon. Secondly, boron is a trivalent metal and is the smallest metalloid. It behaves like a metal when forming oxides, like boron trioxide (B_2O_3), and salts, such as boron sulphate ($B_2(SO_4)_3$), but it behaves like a non-metal when forming acids, such as boric acid (H_3BO_2).[iv]

Because of its vacant p-orbital, boron, and many of the compounds in which it is incorporated, are electron-deficient and thus have a high affinity for electrons. Fisher, *et al*. believe that many of the physiological activities displayed by boronated complexes are the result of competitive Lewis acid/base reactions between different base adducts. Their findings suggest that molecules with B-N dipolar bonds as functional groups have a tendency to interact with important enzyme active sites through noncovalent interactions that bring the boronated functional groups in proximity with the Lewis base active sites of some enzymes.[v] Additionally, the charge distributions of boronated compounds allow for non-covalent interactions that are necessary for the formation of transient interactions with protein docking sites. Finally, the hydrophobic behavior of boronated compounds can be therapeutically manipulated to aid in the design of thermodynamically efficient drugs.[vi] Therefore, the incorporation of boron into pharmaceuticals could lead to a generation of drugs that could interact with targets that are not readily accessible to carbon-based compounds.

1.2 Boron Neutron Capture Therapy

Of particular interest is the use of boronated molecules in an alternative form of cancer therapy called boron neutron capture therapy (BNCT). BNCT involves a binary process with two components that are non-lethal when separated: nonradioactive boron-

10 (^{10}B) and nonionizing neutron radiation. However, when ^{10}B absorbs (captures) one of these slow, low-energy neutrons, an excited boron-11 (^{11}B) is produced, which spontaneously fissions to yield a $^{7}Li^{3+}$ particle, a $^{4}He^{2+}$ particle, and 2.4 MeV of energy.[vii] This boron neutron capture reaction (BNCR) occurs over a distance equivalent to the diameter of one cell; therefore, the lethality of the released energy is primarily limited to the boron-containing cells. Theoretically, this is a highly selective form of treatment that targets tumor cells while sparing the surrounding healthy cells.[viii]

In order for BNCT to be established as a clinically safe and effective treatment, high doses of boronated molecules must be preferentially delivered to tumor cells instead of healthy cells. Two considerations must be made in designing efficient boron-delivery agents. Firstly, boronated drugs must be tumor-selective. Boron must be delivered in high levels to tumor cells, while only accumulating in low levels in healthy cells. A therapeutic dose would require 10^9 atoms of ^{10}B per tumor cell, which is about 30 μg of ^{10}B per gram of tumor throughout the irradiation period, and a neutron fluence of around 10^{12} neutrons per cm^2.[ix] Potential boron carriers such as boron-containing porphyrins, amino acids, nucleosides, and low-density lipoproteins have been explored. However, the optimal delivery agent has yet to be developed, and clinical administration of boron for BNCT remains limited to L-4-(dihydroxyboryl)phenylalanine and the sodium salt of thioborane anion.[x]

Secondly, once boron is delivered to a tumor cell, it must be efficiently taken up by the cell and remain there in therapeutic quantities, as described above, until the radiation treatment. The lethal effects of ^{10}B located in the nucleus are greater than that of ^{10}B in the cytoplasm or bound to the cell membrane due to the breaking of DNA's

double-stranded structure upon the release of $^{7}Li^{3+}$, $^{4}He^{2+}$, and 2.4 MeV of energy during the BNCR.[xi] Potential methods for localizing boron within DNA include nucleosides, DNA alkylating agents, DNA groove binders, and DNA intercalators. However, these various strategies possess no innate selectivity for tumor cells over normal cells and must be selectively delivered by some tumor cell-targeting agent as previously discussed. Nonetheless, understanding the thermodynamics of boronated molecules' interactions with DNA is essential for the rational drug design of boron-containing molecules used in BNCT and other DNA-targeting therapies.

1.3 Intercalation

In addition to BNCT, DNA is the intracellular target of many anticancer, antiviral, and antibiotic drugs.[xii] It is therefore valuable to develop drugs that are sequence- and structure-specific to target different regions of DNA *in vivo* that can then influence gene activity and ultimately cause cell death. Understanding the interactions of boronated drugs with DNA is essential for understanding how they work. Thus, it is also crucial for the development of knowledge that can guide the synthesis of new boronated compounds with enhanced selectivity and increased efficiency. Among the different schemes for inserting drugs within DNA, intercalation poses the greatest potential in terms of cell lethality for BNCT because, not only is DNA damage caused by the BNCR, the vital structure of DNA is additionally distorted by the preliminary interactions of the intercalant molecule with the unwound helix.

DNA intercalation is a process in which flat, heteroaromatic ring systems insert between adjacent base pairs and are stabilized by π-π stacking[xiii] and dipole-dipole[xiv] interactions between the drug and the nucleobases. In order for the intercalating molecule

to fit between adjacent base pairs, the DNA helix must deviate from its original configuration to make room for the molecule to move in. The helix unwinds, extends, and stiffens as a result of the base pairs and backbone untwisting to accommodate the intercalant.[xv] The base pairs separate, and the spacing of phosphate groups in the backbone increases as the helix lengthens by about one base pair, which is approximately 3.4 Å.[xvi] Therefore, to understand the driving forces behind DNA intercalation and what causes the overall binding affinity and specificity of a drug or class of drugs, detailed thermodynamic data describing these reactions is needed. Ultimately, this information will be used to guide rational drug design to improve DNA-targeted drug specificity and efficiency.

1.4 Drug-DNA Binding Free Energy and Intermolecular Forces

In order to accurately describe the driving forces behind drug-DNA complex formation, it is important to calculate the observed binding free energy (ΔG_{obs}) of a complex. The binding free energy of an intercalation process has five contributors: the conformational transitions in the DNA and intercalator (ΔG_{conf}), the free energy cost for the restriction of rotational and translational freedom of the intercalating molecule (ΔG_{r+t}), the hydrophobic contribution (ΔG_{hyd}), the polyelectrolyte contribution (ΔG_{pe}), and the contribution of all other molecular interactions (ΔG_{mol}). All of these factors can be added together to describe the observed binding free energy of a drug-DNA complex:[xvii]

$$\Delta G_{obs} = \Delta G_{conf} + \Delta G_{r+t} + \Delta G_{hyd} + \Delta G_{pe} + \Delta G_{mol}. \quad (1)$$

For a stable drug-DNA complex to form, these five energetic components must combine to result in a net negative binding energy. At least two of the energy

contributions are unfavorable. A positive value for ΔG_{r+t} is the entropic cost of forming a bimolecular complex from two separate reactants, and it results in a decrease in translational and rotational degrees of freedom. A positive value for ΔG_{conf} arises from the energetic cost of conformational changes in the DNA that are necessary to form an intercalation cavity for the intercalant to insert within the DNA and interact with the bases. This is energetically unfavorable because adjacent base pairs must unstack as the helix unwinds and lengthens, costing the complex free energy.[xviii]

In order for DNA-drug interactions to occur, these energetically unfavorable contributions to the observed binding energy must be outweighed by the energetically favorable contributions of the ΔG_{hyd}, ΔG_{pe}, and ΔG_{mol}. The free energy contribution of the hydrophobic transfer process, ΔG_{hyd}, is negative with values of a large magnitude. This is expected because intercalants (and groove binders) feature aromatic rings that are hydrophobic. Thus, their transfer from solution into the interior of a DNA helix is very energetically favorable.[xix] The energetic contribution from the polyelectrolyte effect, ΔG_{pe}, is favorable because it arises from the release of condensed counterions from the DNA when a complex is formed with the intercalant. Because the phosphate groups in the backbone of DNA have a negative charge, DNA is a polyanion. Therefore, when DNA is in solution, it sequesters cations, such as sodium and potassium, around the phosphate group in the backbone, which help to reduce the net charge and stabilize the helix. The interaction of a positively-charged drug with DNA would thus cause one or more of the cations around the phosphate group to be expelled because the intercalant acts as a competing method of neutralizing the backbone.[xx]

Finally, free energy contributions of the noncovalent interactions that occur once the intercalator is inside the complex, ΔG_{mol}, are also energetically favorable. Once the intercalant is transferred from solution into its binding site, weak noncovalent interactions, such as hydrogen bond formation, van der Waals interactions, electrostatic bond formation, dipole-dipole interactions, and induction and dispersion forces, occur between the drug and the DNA.[xxi] These forces act to stabilize the complex, resulting in negative free energy values. Based on analysis of observed binding free energies of the DNA intercalators ethidium and propidium, Ren, *et al*., suggest that the free energy contribution of ΔG_{mol} is most important in obtaining an overall negative ΔG_{obs} because the other four contributions balance each other out.[xxii] Therefore, due to its importance in contributing to an overall negative ΔG_{obs}, this research is focused on calculating the ΔG_{mol} of boronated intercalants.

1.5 Intermolecular Forces and Calculating ΔG_{obs}

While the nature of the formation and breaking of covalent bonds is very well understood and accurately described using computational techniques, the nature of noncovalent interactions is not as clearly understood. Understanding the role of noncovalent interactions in biological systems, such as DNA and DNA-ligand complexes, is very important because they play integral roles in the overall stabilization of these systems. Among the most important noncovalent interactions involved in determining the biomolecular structure of nucleic acid complexes with ligands are hydrogen bonding, π-π stacking, and dispersion interactions.[xxiii] Hydrogen bonds are attractive intermolecular interactions that arise due to electrostatic interactions and bond polarization between an electronegative atom and a hydrogen atom. DNA's helical

structure is largely made possible by the hydrogen bonds that exist between complimentary base pairs on the adjacent strands. Two hydrogen bonds exist between adenine and thymine, while three hydrogen bonds exist between guanine and cytosine.

Stacking interactions are an attractive interaction between aromatic rings that result from overlapping π clouds and are governed by dispersion forces. Dispersion forces are the weakest intermolecular force and occur between uncharged molecules. They arise due to a momentary buildup of charge, or dipoles, between molecules in close proximity; this occurs when atoms experience a momentary uneven distribution of electrons around the nucleus.

In order to investigate the role of noncovalent interactions to the overall observed binding free energy using quantum chemistry, the ΔG_{mol}, or interaction energy, must be calculated using high level *ab initio* methods such as MP2 and CCSD(T), which will be discussed shortly. A 2007 study by Lin, *et al.*, examined the role of the four-ring aromatic compound ellipticine as a DNA intercalant by calculating its interaction energy within a DNA complex using the following equation:[xxiv]

$$E_{interaction} = E_{whole\ complex} - E_{ellipticine} - E_{4\text{-}nucleobase\ complex}. \quad (2)$$

This research utilizes a similar equation to calculate the interaction energies of intercalants within single-stranded DNA complexes composed of two bases as well as double-stranded DNA complexes with four bases, making two base pairs. For single-stranded complexes, the following equation is used:

$$E_{interaction} = (E_{whole\ complex} - E_{2\text{-}nucleobase\ complex} - E_{ligand})*627.5095, \quad (3)$$

where 627.5095 kcal/mol-hartree is the conversion factor used to convert units into kcal/mol. Similarly, the equation used to calculate the interaction energy for double-stranded complexes is as follows:

$$E_{interaction} = (E_{whole\ complex} - E_{left\ strand} - E_{right\ strand} - E_{ligand})*627.5095. \quad (4)$$

To assess the accuracy of the model chemistry used, the DNA binding energy of the hydrogen bonds holding each DNA strand together can be calculated and compared to expected energy values. Each hydrogen bond should contribute 8-15 kcal to the stabilization of the DNA complex; therefore, this can be used to calibrate the accuracy of the double-stranded model used in this study. If the observed DNA binding energies fall within the expected range based on the number of hydrogen bonds in each complex, the system can be considered to be accurately modeled. The DNA binding energy can be calculated using:

$$E_{interaction} = (E_{whole\ complex} - E_{left\ strand} - E_{right\ strand})*627.5095. \quad (5)$$

Complexes with adenine and thymine should yield a binding energy between 32-60 kcal; complexes with guanine and cytosine only should yield a binding energy between 48-90 kcal; and complexes with all four nucleobases should yield a binding energy between 40-75 kcal.

1.6 Appropriate Computational Methods for Drug-DNA Interactions

In order to most accurately report the interaction energies of boronated intercalants, several computational methods were used and their values were compared to those produced by the most accurate method available, considering the computational resources of this research group. The second order Møller-Plesset perterbation theory (MP2)[xxv] is a Wave Functional Theory (WFT) method and is one of the most popular

methods used for noncovalent interactions. MP2 takes into account energy contributions from the ground state wavefunction plus those from the configuration interaction wavefunctions for doubly excited states. In other words, it takes into account electrons that avoid each other through double excitations that cause correlation energy, which is the energy associated with electrons moving into excited states.

When compared to the benchmark method (Coupled Cluster Singles, Doubles, and Triples), MP2 accurately estimates the interaction energies of hydrogen-bonded systems and yields "reasonable" interaction energies using medium and small basis sets.[xxvi] However, MP2 is not an accurate method for stacking calculations (calculations for dispersion-bound systems) but gives reasonable results for systems at long-range distances. Due to the constraints of our computational resources, MP2 is the cheapest (in terms of time and memory) and most accurate method available.

On the other hand, SVWN[xxvii,xxviii] is a Density Functional Theory (DFT) method that has been proven to accurately estimate interaction energies for aromatic systems. DFT methods only take into account the ground state determinant but add integrals to the Hamiltonian to make up for their inability to take into account the exchange and correlation energy. The problem with DFT that causes its unsatisfactory description of intermolecular forces lies in the approximation made by these added functionals. DFT functionals must approximate the unknown exchange correlation potential, and this necessary approximation makes DFT methods generally less accurate. Although DFT methods work well in some cases, they are not always reliable. Even though DFT methods are generally inaccurate for dispersion, SVWN is a DFT method that provides accurate estimations for metals and, surprisingly, π systems (aromatic systems with

dispersion-dominated stacking interactions).[xxix] Additionally, the method HCTH[xxx] is a DFT method that is generally accurate for modeling electrostatic forces and systems with dispersed electron densities.

The most accurate method available in computational chemistry is the method Coupled Cluster Singles, Doubles, and Triples, CCSD(T).[xxxi] CCSD(T) is the industry standard and accounts for more than 99% of electron correlation energy by taking into account energy contributions from the ground state wavefunction plus those from the configuration interaction wavefunctions for singly, doubly, and triply excited states. Because CCSD(T) has been established as the most accurate method for interaction energies when used with an extended basis set, it provides benchmark data that can be used to evaluate the accuracy of computationally cheaper methods such as WFT and DFT methods. However, CCSD(T) is extremely expensive in terms of time and memory; therefore, computationally cheaper methods, such as Coupled Cluster Singles and Doubles[xxxii] (CCSD), exist and provide results of similar accuracy. CCSD is the most accurate method available to this research group. Therefore, in this research, CCSD is used as the standard of accuracy to which results provided by MP2 and SVWN are compared to evaluate accuracy.[xxxiii]

Finally, for large systems, methods such as ONIOM can be used to apply different levels of theory, and thus accuracy, to different parts of the system. The portion of the system in the higher level is treated with a method of a higher level of accuracy, while the portion of the system in the lower level is treated with a method of a lower level of accuracy. This allows for less computational resources to be used on an area of the system that is not as important to consider when calculating interaction energies. In this

case, a lower accuracy method is applied to the DNA backbone, while a higher accuracy method is applied to the nucleobases and intercalating molecule.

1.7 Model Boronated Intercalants

The majority of this research focuses on the binding of borazine compared to that of benzene within single-stranded and double-stranded DNA complexes (Figure 1). Borazine is a planar aromatic molecule chosen for this study because it is both boronated and comparable to the aromatic structures found in many pharmaceuticals. Its observed interactions are compared to those of benzene, which is a conventional, nonpolar, organic molecule. Borazine is isoelectronic with benzene and similar in structure except that it consists of alternating boron and nitrogen atoms, thus creating alternating centers of positive (B) and negative (N) charge. Rings such as benzene interact non-covalently through induction and dispersion forces; thus, the inclusion of heteroatoms, such as boron and nitrogen, can improve the ring binding.

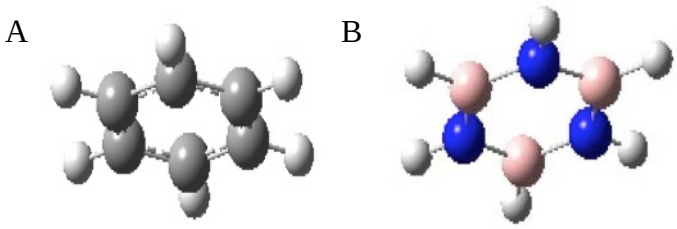

Figure 1. The use of benzene as a model organic intercalant and borazine as a model boronated intercalant. Carbon atoms are shown in grey; hydrogen atoms are shown in white; boron atoms are shown in pink; and nitrogen atoms are shown in blue. Because of their comparable size and structure, benzene (A) and borazine (B) are used as model intercalants in order to characterize the interaction of boronated intercalants within DNA as opposed to that of organic intercalants.

Therefore, because borazine possesses alternating charges within the ring, resulting in a polarization of charge, it was originally expected that borazine would

display different interactions with the nitrogenous bases within the DNA complex than those of benzene, which is composed of carbon and hydrogen only. Previous research in this group investigated the solvent interactions of the boronated aromatic molecule borazine compared to those of the conventional organic molecule benzene. In a simplified intercalation model, organic molecules were most often observed to preferentially interact with a boronated molecule rather than another organic molecule.[xxxiv] Thus it was originally expected that borazine would demonstrate improved interactions with the organic nucleobases of DNA compared to benzene.

Additionally, the presence of a dipole within the intercalant presents the possibility of improvement of intermolecular forces by increasing the chances that the charges located in the ring of the intercalant will successfully align with charges located in the DNA bases. The symmetry of alternating localized charges within a borazine molecule may make it more difficult for partial charges in the boronated intercalant to align with charges in the bases. Therefore, interactions of a hybrid intercalant, designed to have a dipole, are also compared to the interactions of benzene and borazine in order to investigate a possible improvement in intermolecular forces within the drug-DNA complexes (Figure 2).

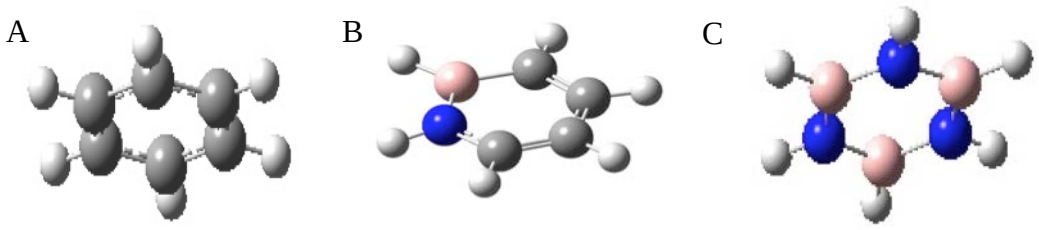

Figure 2. The use of a hybrid intercalant to investigate possible improved intermolecular forces compared to those of benzene and borazine. In order to investigate interaction strength of an intercalant with a dipole, the interactions of a hybrid intercalant (B) are compared to the interactions of benzene (A) and borazine (C).

2. Methods

All DNA complexes were isolated from crystal structures located in the Protein Data Bank (PDB ID: 3HF6[xxxv] for single-stranded structures and PDB ID: 3MFK[xxxvi] or 2WI2[xxxvii] for double-stranded structures). Because charged electron densities are difficult to describe using quantum mechanics, DNA complexes were altered by adding a hydrogen atom to the phosphate groups in the DNA backbone in order to neutralize the backbone's net negative charge and to obtain reliable computational data from which to build upon later. The added hydrogen was later removed when interaction energies of charged double-stranded complexes were computed.

After the DNA complex was prepared for optimization, a benzene intercalant was then added between the nucleobases, and the complexes were optimized using SVWN/6-31+G* for the single-stranded complexes and ONIOM(SVWN/3-21G:AM1) for the double-stranded complexes. Double-stranded complexes that were optimized using ONIOM(SVWN/6-31G:AM1) include ATTA, ATTAb, ATATb, and ATGC as well as ATAT and ATGC with the hybrid intercalant. Optimized complexes with benzene were used as a starting point for optimizing complexes with borazine or a hybrid intercalant by replacing the benzene intercalant in the optimized complex with a borazine or the hybrid molecule. The complex was then re-optimized with the borazine or hybrid intercalant. Interaction energies were computed from optimized complexes with both benzene and borazine intercalants and later with the hybrid intercalant.

Counterpoise-corrected interaction energies for single-stranded uncharged complexes were computed using MP2 and CCSD with a basis set of 6-31+G* (ONIOM was used with AM1 for the DNA backbone), SVWN with 6-31+G*, and MP2, SVWN,

and HCTH with a basis set of 6-311+G*. Counterpoise-corrected interaction energies for double-stranded uncharged and charged complexes were computed using MP2 with a basis set of 6-31+G* (ONIOM was used with AM1 for the DNA backbone). As a test for accuracy, DNA binding energies of double-stranded complexes were also calculated in the same way as above. All calculations were run using Gaussian '03[xxxviii] on an Altix Cluster using 4-8 processors and 4-8 GB of memory per job.

3. Results and Discussion

3.1 Single-Stranded Models

In order to investigate the interaction strength of boronated aromatic intercalants versus organic aromatic intercalants, interaction energies were calculated in kcal/mol for borazine and benzene intercalants within small single-stranded DNA complexes using the methods SVWN and MP2 with a basis set of 6-31+G*. Complexes tested are as follows: adenine/adenine (AIA, AIAb), adenine/guanine (AIG, AIGb), adenine/thymine (AIT, AITb), and cytosine/guanine (CIG, CIGb). The abbreviated notation AIA represents an adenine/adenine complex with a benzene intercalant; the corresponding notation AIAb represents an adenine/adenine complex with a borazine intercalant (Figure 3). All single-stranded abbreviations follow this same pattern.

A B

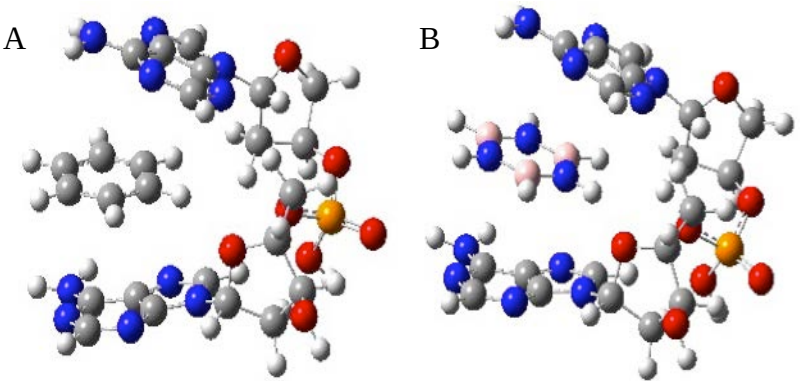

Figure 3. Single-stranded structures with a benzene or borazine intercalant. Oxygen atoms are shown in red, and phosphorus atoms are shown in orange. Pictured are single-stranded adenine/adenine complexes with benzene (A) and borazine (B) intercalants. Structures of all single-stranded complexes can be found in Appendix 1.

Among the four complexes observed, interaction energies ranged from -10.99 kcal/mol (CIG) to -17.67 kcal/mol (AIAb) for SVWN and from -11.51 kcal/mol (CIG) to -20.54 kcal/mol (AIA) for MP2. SVWN generally indicated that borazine interacts more strongly within the single-stranded complexes, while MP2 generally indicated that benzene interacts more strongly (Table 1). The CIG complex was the one exception to this trend because both SVWN and MP2 indicated that borazine has a stronger interaction. Overall, these initial calculations indicate a conflicting trend as to which intercalant interacts more strongly with the organic nucleobases of the single-stranded DNA complex. *Note: A negative sign indicates attraction, and a positive sign indicates repulsion. Therefore, larger negative values indicate stronger binding energies.

Table 1. SVWN and MP2/6-31+G* results for single-stranded counterpoise-corrected interaction energies. Interaction energies are reported for single-stranded DNA complexes with an intercalant; complexes with benzene intercalants are highlighted in grey, and complexes with borazine intercalants are white. SVWN consistently yields larger negative values for complexes with borazine while MP2 yields larger negative values for all complexes with benzene except for the CIG complex. All calculations are performed with 6-31+G*, and all calculations are quoted in kcal/mol.

Complex	SVWN	MP2
Adenine_Benzene_Adenine (AIA)	-11.79	-20.45
Adenine_Borazine_Adenine (AIAb)	-17.67	-17.71
Adenine_Benzene_Thymine (AIT)	-11.61	-17.48
Adenine_Borazine_Thymine (AITb)	-11.98	-13.72
Adenine_Benzene_Guanine (AIG)	-12.22	-19.41
Adenine_Borazine_Guanine (AIGb)	-12.66	-14.82
Cytosine_Benzene_Guanine (CIG)	-10.99	-11.51
Cytosine_Borazine_Guanine (CIGb)	-13.44	-11.88

To see if a better description of atomic orbitals would help distinguish a consistent trend in interaction strength, the previous calculations, as well as calculations for the remaining single-stranded complexes, were run again using SVWN and MP2 with the larger basis set 6-311+G*. The remaining complexes include adenine/cytosine (AIC, AICb), cytosine/cytosine (CIC, CICb), cytosine/guanine (CIG, CIGb), cytosine/thymine (CIT, CITb), guanine/guanine (GIG, GIGb), guanine/thymine (GIT, GITb), and thymine/thymine (TIT, TITb). Interaction energy values ranged form -9.68 kcal/mol (CIT) to -18.58 kcal/mol (GIGb) for SVWN and from -10.97 kcal/mol (CITb) to -25.80 kcal/mol (GIG) for MP2. Using 6-311+G*, SVWN again indicated that borazine interacts more strongly within the single-stranded complexes, while MP2 indicated that benzene interacts more strongly within every complex (Table 2). Thus, the same conflicting trend is seen using the larger basis set.

Table 2. SVWN and MP2/6-311+G* results for single-stranded counterpoise-corrected interaction energies. Interaction energies are reported for all single-stranded DNA complexes with an intercalant using 6-311+g*. SVWN consistently yields larger negative values for complexes with a borazine intercalant (grey), and MP2 consistently yields larger negative values for complexes with a benzene intercalant (white). All calculations are quoted in kcal/mol.

Complex	SVWN	MP2		Complex	SVWN	MP2
AIA	-11.88	-21.84		CIG	-11.65	-13.71
AIAb	-17.68	-19.05		CIGb	-13.88	-12.48
AIT	-11.68	-18.71		CIT	-9.68	-13.83
AITb	-11.95	-14.53		CITb	-15.17	-10.97
AIG	-12.42	-20.66		GIT	-10.43	-17.66
AIGb	-12.92	-15.43		GITb	-14.94	-14.56
AIC	-9.89	-17.01		GIG	-16.21	-25.80
AICb	-12.65	-12.96		GIGb	-18.58	-20.16
CIC	-10.32	-15.42		TIT	-10.25	-14.77
CICb	-14.49	-13.03		TITb	-15.87	-12.71

Because a conflicting trend was again seen using a larger basis set, interaction energies for all single-stranded uncharged complexes were calculated using the DFT method HCTH, which is generally accurate for modeling electrostatic forces and systems with dispersed electron densities, with the basis set 6-311+G*. HCTH consistently produced positive interaction energies, ranging from 13.24 kcal/mol (AIG) to 32.41 kcal/mol (CIG) and thus indicating repulsion, rather than attraction, of both intercalants within every complex (Table 3). Therefore, the discrepancy between these results and the previous MP2 results suggest that HCTH is not an accurate method to use for this type of calculation involving intercalation in a small DNA model. Furthermore, because HCTH is considered generally accurate for modeling electrostatic forces, its production of positive interaction energy values suggests that the system is dominated by induction and dispersion forces rather than electrostatic forces.

Table 3. HCTH/6-311+G* results for single-stranded counterpoise-corrected interaction energies. Interaction energies are reported for all single-stranded DNA complexes with an intercalant using 6-311+G*. HCTH yields positive interaction energy values for every intercalation complex. All calculations are quoted in kcal/mol.

Complex	HCTH		Complex	HCTH
AIA	18.19		CIG	32.41
AIAb	21.70		CIGb	17.59
AIT	19.38		CIT	13.85
AITb	17.39		CITb	13.90
AIG	13.24		GIT	20.74
AIGb	14.54		GITb	21.95
AIC	20.57		GIG	20.26
AICb	20.62		GIGb	20.66
CIC	14.00		TIT	15.90
CICb	17.92		TITb	18.22

For added accuracy in distinguishing a trend as to which intercalant interacts strongest within small single-stranded DNA models, interaction energies were calculated for all single-stranded complexes using the most accurate method available considering our computational resources, Coupled Cluster Singles and Doubles (CCSD). CCSD has been established as one of the most accurate method for interaction energies when used with an extended basis set. Therefore, CCSD provides benchmark data that can be used to evaluate the accuracy of computationally cheaper methods such as WFT and DFT methods (in this case, MP2 and SVWN, respectively).[xxxix]

Previous work in our group demonstrates that similar interaction energy values can be obtained for an intercalant within a small single-stranded DNA model using the basis sets 6-31+G* and 6-311+G*.[xl] Therefore, the smaller basis set 6-31+G* was used for all CCSD calculations and all later calculations. Interaction energy values ranged

from -1.35 kcal/mol (CIG) to -13.26 kcal/mol (GIG). CCSD/6-31+G* reveals a trend in which benzene interacts the strongest with the majority (7 of 10) of single-stranded complexes (Table 4). Because CCSD indicates that benzene has a stronger interaction and thus agrees with MP2 for the majority of the complexes, it is concluded as the more accurate method for this type of system and allows the use of MP2 for all later calculations.

Table 4. CCSD/6-31+6* results for single-stranded counterpoise-corrected interaction energies. Interaction energies are reported for all single-stranded DNA complexes with an intercalant using CCSD/6-31+g*. CCSD yields larger negative interaction energy values for seven of ten single-stranded complexes with a benzene intercalant (grey). Three of ten complexes yield larger negative interaction energy values for complexes with a borazine intercalant (white). All calculations are quoted in kcal/mol.

Complex	CCSD		Complex	CCSD
AIA	-10.39		CIG	-1.35
AIAb	-10.64		CIGb	-7.46
AIT	-9.47		CIT	-7.92
AITb	-8.97		CITb	-6.83
AIG	-11.42		GIT	-8.38
AIGb	-9.51		GITb	-8.80
AIC	-7.71		GIG	-13.26
AICb	-7.58		GIGb	-12.16
CIC	-8.55		TIT	-8.33
CICb	-8.41		TITb	-7.64

3.2 Double-Stranded Models

Next, to further observe the interaction strength of boronated aromatic intercalants versus organic aromatic intercalants within small DNA models, interaction energies were calculated in kcal/mol for borazine and benzene intercalants within small, uncharged double-stranded DNA complexes using MP2 with the basis set 6-31+G*. Complexes

tested are as follows: guanine/cytosine-guanine/cytosine (GCGC, GCGCb), guanine/cytosine-cytosine/guanine (GCCG, GCCGb), adenine/thymine-adenine/thymine (ATAT, ATATb), adenine/thymine-thymine/adenine (ATTA, ATTAb), adenine/thymine-cytosine/guanine (ATCG, ATCGb), and adenine/thymine-guanine/cytosine (ATGC, ATGCb). The abbreviated notation GCGC represents a guanine/cytosine-guanine/cytosine complex with a benzene intercalant; the corresponding notation GCGCb represents a guanine/cytosine-guanine/cytosine complex with a borazine intercalant (Figure 4). All double-stranded abbreviations follow this same pattern.

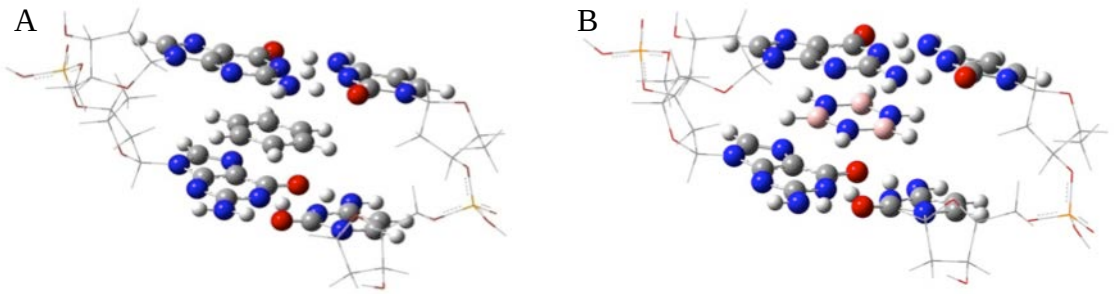

Figure 4. Double-stranded structures with a benzene or borazine intercalant. Pictured are double-stranded guanine/cytosine-guanine/cytosine complexes with benzene (A) and borazine (B) intercalants. Structures of all double-stranded complexes can be found in Appendix 2.

Interaction energy values produced with MP2/6-31+G* ranged from -15.83 kcal/mol (ATCGb) to -32.57 kcal/mol (ATGC). MP2 indicates a general trend in which benzene interacts more strongly within all double-stranded complexes except the ATAT complex (Table 5). To assess the accuracy of this double-stranded model, DNA binding energies were calculated in kcal/mol for each double-stranded complex. All binding energy values fell within the expected ranges, and thus each complex was determined to have been accurately modeled.

Table 5. MP2/6-31+G* results for uncharged, double-stranded counterpoise-corrected interaction energies. Intercalant interaction energies for all uncharged double-stranded DNA complexes using MP2/6-31+G* yield larger negative values for complexes with a benzene intercalant (grey) than the corresponding complexes with a borazine intercalant (white) except for the adenine/thymine-adenine/thymine (ATAT) complex. MP2 indicates a larger negative interaction energy for the borazine intercalant within the ATAT complex than for the benzene intercalant. All DNA binding energies for uncharged double-stranded DNA complexes using MP2/6-31+G* fall within the expected ranges, based on each complexes' number of hydrogen bonds. All calculations are quoted in kcal/mol.

MP2/6-31+G*	**Interaction Energies**	
Complex	**Intercalant**	**DNA**
GCGC	-28.43	-78.54
GCGCb	-24.25	-77.74
GCCG	-27.81	-78.38
GCCGb	-24.75	-75.53
ATAT	-25.81	-50.93
ATATb	-28.34	-48.28
ATTA	-31.90	-44.09
ATTAb	-27.60	-45.23
ATCG	-27.98	-61.67
ATCGb	-15.83	-59.67
ATGC	-32.57	-62.97
ATGCb	-23.39	-66.11

To investigate the interaction strength of boronated versus organic intercalants within DNA systems with a charged backbone, interaction energies were calculated in kcal/mol using MP2/6-31+G* for all double-stranded complexes in which the phosphate group of the backbone was left charged. Interaction energy values ranged from -15.47 kcal/mol (ATCGb) to -32.76 kcal/mol (ATGC). MP2 again indicates that benzene interacts more strongly within all double-stranded complexes except the ATAT complex (Table 6). Furthermore, all charged and uncharged complexes demonstrate a difference in intercalant interaction energy strength of about one-fourth kcal, thus suggesting that the

negatively-charged DNA backbone is of little importance when modeling the interaction strength of boronated intercalants.

Table 6. **MP2/6-31+G* results for charged, double-stranded counterpoise-corrected interaction energies.** Interaction energies for all charged double-stranded DNA complexes using MP2/6-31+G* yield larger negative values for complexes with a benzene intercalant (grey) than those with a borazine intercalant (white) except for the ATAT complex. MP2 indicates a larger negative interaction energy for the borazine intercalant within the ATAT complex than for the benzene intercalant. All calculations are quoted in kcal/mol.

MP2/6-31+G*	Intercalant Interaction Energies	
Complex	**Uncharged**	**Charged**
GCGC	-28.43	-28.65
GCGCb	-24.25	-24.04
GCCG	-27.81	-28.07
GCCGb	-24.75	-24.61
ATAT	-25.81	-25.89
ATATb	-28.34	-28.10
ATTA	-31.90	-32.06
ATTAb	-27.60	-27.69
ATCG	-27.98	-28.19
ATCGb	-15.83	-15.47
ATGC	-32.57	-32.76
ATGCb	-23.39	-23.22

3.3 Double-Stranded Models with a Hybrid Intercalant

To examine possible improvement of interaction strength of boronated intercalants due to the presence of a dipole within the intercalating molecule, interaction energies were calculated for the hybrid intercalant within charged, double-stranded DNA complexes using MP2 and the basis set 6-31+G*. Energy values range from -24.60 kcal/mol (GCGC) to -34.58 kcal/mol (ATTA). The energy values for hybrid intercalant interaction strength within all double-stranded complexes are higher (more negative) than those of borazine, indicating improved interactions compared to the borazine intercalant

(Table 7). The energy values of the hybrid intercalant within the GCGC, GCCG, ATCG, and ATGC complexes are lower than those of the borazine intercalant within the same charged complexes; however, the energy values of the hybrid intercalant within the ATTA and ATAT complexes exceed those of the benzene intercalant within the same charged complexes. These results suggest that an intercalant design in which the heteroatom position creates a dipole will more successfully interact with DNA bases than a design in which the symmetry of localized charges eliminates the possibility of a dipole and thus makes it more difficult for the localized charges of the intercalant to align with localized charges in the DNA bases.

Table 7. **MP2/6-31+G* results for counterpoise-corrected interaction energies of charged, double-stranded complexes with a hybrid intercalant.** Interaction energies for all charged double-stranded DNA complexes with a hybrid intercalant using MP2/6-31+G* yield larger negative values than those of a borazine intercalant in the same complex. All interaction energies for complexes with a hybrid intercalant yield smaller negative values than those a benzene intercalant in the same complex, except for the ATAT and ATTA complexes. MP2 indicates a larger negative interaction energy for the hybrid intercalant within the ATAT and ATTA complexes than for both the benzene and borazine intercalants. All calculations are quoted in kcal/mol.

MP2/6-31+G*	**Intercalant**		
Complex	**Hybrid**	**Benzene**	**Borazine**
GCGC	-24.60	-28.65	-24.04
GCCG	-27.72	-28.07	-24.61
ATCG	-27.55	-28.19	-15.47
ATGC	-29.34	-32.76	-23.22
ATTA	-34.58	-32.06	-27.69
ATAT	-28.79	-25.89	-28.10

4. Conclusion

Considering the initial single-stranded calculations produced using SVWN and MP2 with medium- and larger-sized basis sets, a conflicting trend is observed in which SVWN generally reports that borazine has a stronger interaction within the small DNA complexes, while MP2 reports that benzene has stronger interactions. The use of the DFT method HCTH, which is generally accurate for electrostatic forces and systems with dispersed electron densities, reveals that this method is, in fact, inaccurate for small drug-DNA systems due to its production of positive interaction energy values. Additionally, this outcome indicates that the observed system of a boronated intercalant within a small DNA model is dominated by induction and dispersion forces rather than electrostatic forces. Due to this, the interactions of boronated intercalants with the nucleobases greatly depend on the ability of the partial charges within the ring of the intercalant to align with the localized charges in the rings of each nucleobase. Furthermore, the CCSD results match the MP2-produced trend that benzene interacts more strongly with the small DNA complexes than borazine and also confirm that MP2 is more accurate than SVWN for this type of system. This conclusion dictated the use of MP2 for all following double-stranded calculations.

Double-stranded calculations using MP2 with a medium-sized basis set revealed a trend that is generally consistent with the trend produced by the single-stranded calculations. The double-stranded data indicates a trend in which benzene has a stronger interaction within all DNA complexes with an uncharged and a charged backbone, except for the ATAT complex. These results suggest that location further inside the intercalation

cavity, away from the negatively charged phosphate group in the backbone, does not affect the overall trend of borazine's interaction strength within the complexes.

The generally weaker interactions observed in the borazine complexes could be attributed to the symmetry of the borazine molecule. Because of the position of alternating positive and negative charges around the entire ring due to bond polarization, the symmetry of the molecule prevents the production of a dipole within the intercalant. Calculations using MP2 with the medium sized basis set with the hybrid intercalant in the charged, double-stranded DNA complexes revealed a trend in which the interaction strength of the hybrid intercalant in every complex improved from those of the borazine intercalants. This suggests that the presence of a dipole within the intercalating molecule improves the alignment of charges within the intercalant with charges located in the nucleobases.

Additionally, improved binding of the hybrid intercalant compared to the benzene intercalant in two of the double-stranded complexes further suggests that the presence of a dipole in the boronated intercalant could be important in designing a boronated drug with the greatest ability to intercalate DNA. Finally, the observation that the hybrid intercalant displayed improved interactions compared to the benzene intercalant in the ATAT and ATTA complexes, specifically, suggests a possibility for selective-targeting of specific DNA sequences when designing boronated intercalants. However, more detailed calculations are needed to investigate this trend. The repeated deviation of complexes with only adenine and thymine from the general trend could be attributed to the fact that adenine and thymine nucleobases have fewer hydrogen bonds than the guanine and cytosine nucleobases. Complexes with only adenine and thymine have four

hydrogen bonds. Comparatively, complexes with only guanine and cytosine have six hydrogen bonds, and complexes with all four nucleobases have five hydrogen bonds. Thus, because the ATAT and ATTA complexes are less tightly bound than the other double-stranded complexes, they may be able to deform more and better accommodate the intercalant. Overall, the use of boron in intercalating drug design shows promise in enhancing the interaction strength and selectivity of DNA-targeted drugs.

5. Works Cited

1. Patrick, G. *Medicinal Chemistry*. Bios: Scientific Publishers Limited, 2001; 142.
2. Fisher, L.S., McNeil, K., Butzen, J., Holme, T.A. (2000) *J. Phys. Chem.* **104**, 3744-3751.
3. McCoy, M. *Chem. Eng. News* [Online] **2011,** *89*, 12. http://pubs.acs.org/isubscribe/journals/cen/89/i12/html/8912cover3.html (accessed June 7, 2011).
4. Hunter, P. (2009). *EMBO Rep.* **10**, 125-128.
5. Fisher, L.S., McNeil, K., Butzen, J., Holme, T.A. (2000) *J. Phys. Chem.* **104**, 3744-3751.
6. Hunter, P. (2009). *EMBO Rep.* **10**, 125-128.
7. Lesnikowski, Z. J., *et al*. (2005) *Bioorg. Med. Chem.* **13**, 4168-4175.
8. Hawthorne, M. F. (1998) *Mol. Med. Today* **4**, 174-181.
9. Hawthorne, M. F. (1998) *Mol. Med. Today* **4**, 174-181.
10. Lesnikowski, Z. J., *et al*. (2005) *Bioorg Med Chem* **13**, 4168-4175.
11. Hawthorne, M. F. (1998) *Mol. Med. Today* **4**, 174-181.
12. Haq, I. (2002) *Arch. Biochem. Biophys.* **403**, 1-15.
13. Haq, I. (2002) *Arch. Biochem. Biophys.* **403**, 1-15.
14. Long, E.C, Barton, J.K. (1990) *Acc. Chem. Res.* **23**, 273-279.
15. Long, E.C, Barton, J.K. (1990) *Acc. Chem. Res.* **23**, 273-279.
16. Haq, I. (2002) *Arch. Biochem. Biophys.* **403**, 1-15.
17. Ren, J., Jenkins, T.C., and Chaires, J.B. (2000) *Biochemistry* **39**, 8439-8447.
18. Chaires, J.B. (1997) *Bipolymers.* **44**, 201-215.
19. Chaires, J.B. (1997) *Bipolymers.* **44**, 201-215.
20. Haq, I. (2002) *Arch. Biochem. Biophys.* **403**, 1-15.
21. Chaires, J.B. (1997) *Bipolymers.* **44**, 201-215.
22. Ren, J., Jenkins, T.C., and Chaires, J.B. (2000) *Biochemistry* **39**, 8439-8447.
23. Riley, K.E., Hobza, P. (2011) *WIRE.* **1**, 3-17.
24. Lin, I., Lilienfeld, O., Coutinho-neto, M., Tavernelli, I., and Rothlisberger, U. (2007) *J. Phys. Chem. B.* **111**, 14346-14354.
25. Head-Gordon, M., Head-Gordon, T. (1994) *Chem. Phys. Lett.* **220**, 122.

26. Riley, K. E., Hobza, P. (2011) *WIRE*. **1**, 3-17.
27. Slater, J.C. *Quantum Theory of Molecular and Solids*. Vol. 4: *The Self-Consistent Field for Molecular and Solids* (McGraw-Hill, New York, 1974).
28. Vosko, S.H., Wilk, L. Nusair, M. (1980) *Can. J. Phys.* **58**, 1200.
29. Riley, K. E., Hobza, P. (2011) *WIRE*. **1**, 3-17.
30. Boese, A.D., Handy, N.C. (2001) *J. Chem. Phys.* **114**, 5497.
31. Pople, J.A., Head-Gordon, M., Raghavachari, K. (1987) *J. Chem. Phys.* **87**, 5968.
32. Purvis, G.D., Bartlett, R.J. (1982) *J. Chem. Phys.* **76**, 1910.
33. Riley, K.E., Hobza, P. (2011) *WIRE*. **1**, 3-17.
34. Jeans, L. B., Cafiero, M. Unpublished Work.
35. Cianchetta, G., Stouch, T., Yu, W. Shi, Z.-C., Tari, L.W., *et al*. (2010) *Curr Chem Genomics* **4:** 19-26.
36. Babayeva, N.D., Wilder, P.J., Shiina, M., Mino, K., Desler, M., *et al*. (2010) *Cell Cycle* **9:** 3054-3062.
37. Brough, P.A., Barril, X., Borgognoni, J., Chene, P., Davies, N.G.M., *et al*. (2009) *J. Med. Chem.* **52:** 4794.
xxxviii. Gaussian 03, Revision C.02, M. J. Frisch, G. W. Trucks, H. B. Schlegel, G. E. Scuseria, M. A. Robb, J. R. Cheeseman, J. A. Montgomery, Jr., T. Vreven, K. N. Kudin, J. C. Burant, J. M. Millam, S. S. Iyengar, J. Tomasi, V. Barone, B. Mennucci, M. Cossi, G. Scalmani, N. Rega, G. A. Petersson, H. Nakatsuji, M. Hada, M. Ehara, K. Toyota, R. Fukuda, J. Hasegawa, M. Ishida, T. Nakajima, Y. Honda, O. Kitao, H. Nakai, M. Klene, X. Li, J. E. Knox, H. P. Hratchian, J. B. Cross, V. Bakken, C. Adamo, J. Jaramillo, R. Gomperts, R. E. Stratmann, O. Yazyev, A. J. Austin, R. Cammi, C. Pomelli, J. W. Ochterski, P. Y. Ayala, K. Morokuma, G. A. Voth, P. Salvador, J. J. Dannenberg, V. G. Zakrzewski, S. Dapprich, A. D. Daniels, M. C. Strain, O. Farkas, D. K. Malick, A. D. Rabuck, K. Raghavachari, J. B. Foresman, J. V. Ortiz, Q. Cui, A. G. Baboul, S. Clifford, J. Cioslowski, B. B. Stefanov, G. Liu, A. Liashenko, P. Piskorz, I. Komaromi, R. L. Martin, D. J. Fox, T. Keith, M. A. Al-Laham, C. Y. Peng, A. Nanayakkara, M. Challacombe, P. M. W. Gill, B. Johnson, W. Chen, M. W. Wong, C. Gonzalez, and J. A. Pople, Gaussian, Inc., Wallingford CT, 2004.
39. Riley, K.E., Hobza, P. (2011) *WIRE*. **1**, 3-17.
40. Shroyer, M. Ab Initio and DFT Calculations of Increasingly Complex Models of Ligand-Nucleic Acid Binding. B.S. Thesis, Rhodes College, Memphis, TN, 2011.

6. Appendix 1: Single-Stranded DNA Complexes

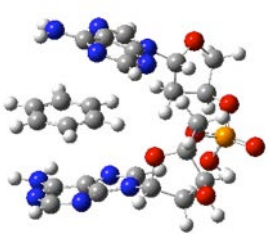

AIA

AIAb

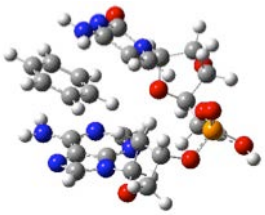

AIC

AICb

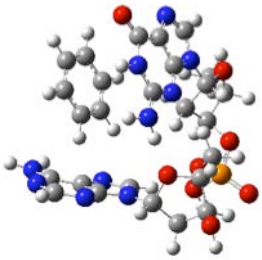

AIG

AIGb

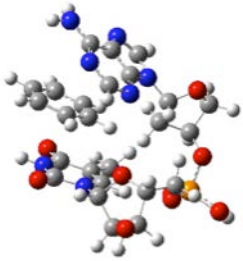

AIT

AITb

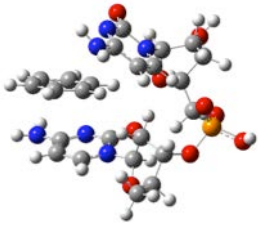

CIC

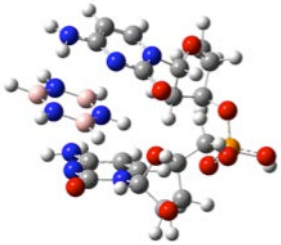

CICb

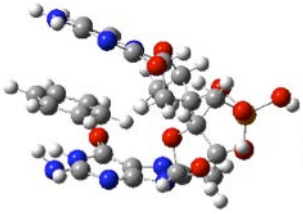

CIG

CIGb

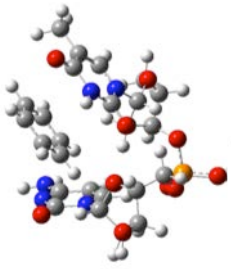

CIT

CITb

GIG

GIGb

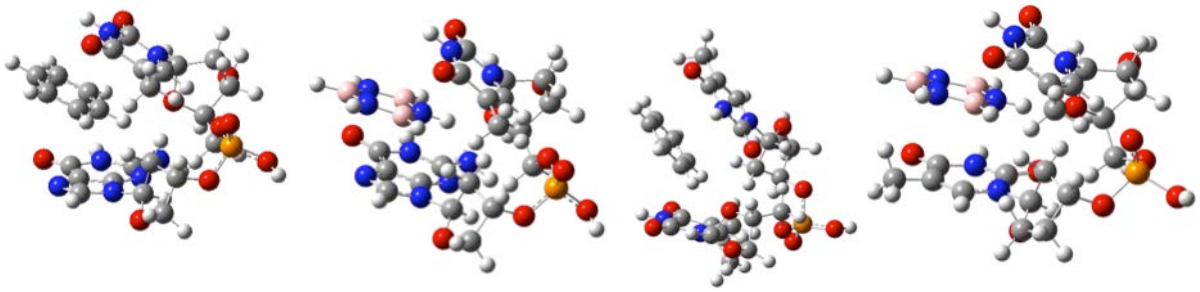

GIT GITb TIT TITb

7. Appendix 2: Double-Stranded DNA Complexes

7.1 Uncharged Double-Stranded Complexes

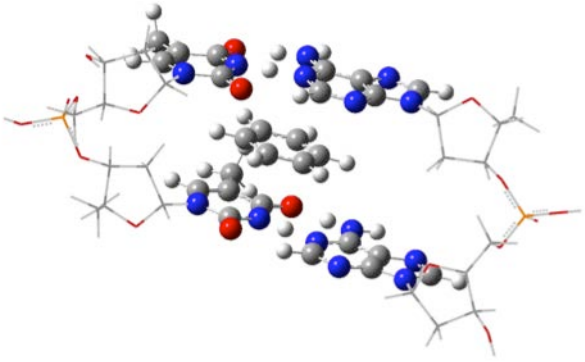

ATAT

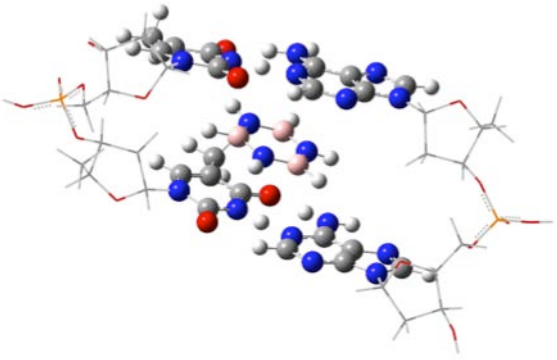

ATATb

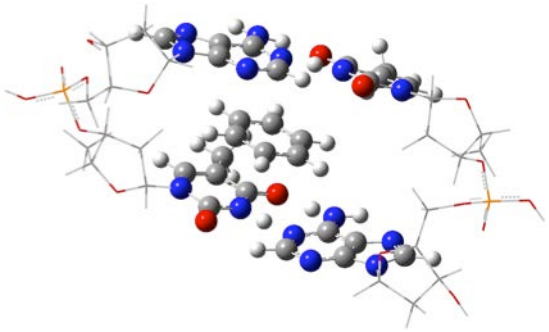

ATTA

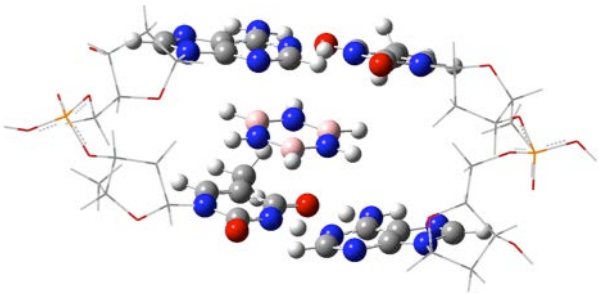

ATTAb

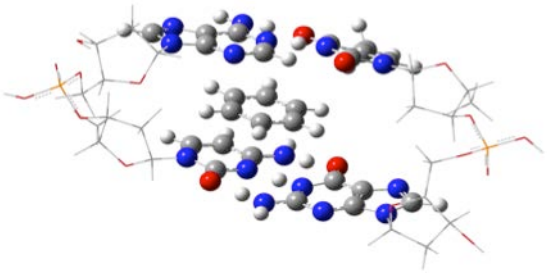

ATCG

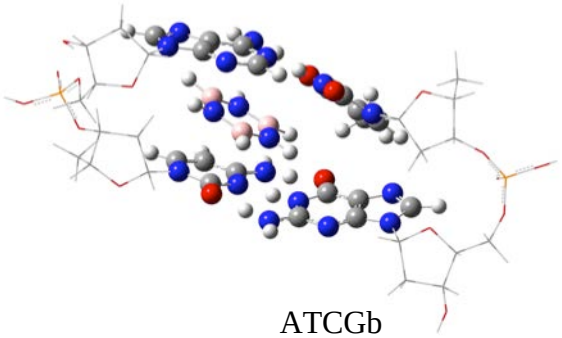

ATCGb

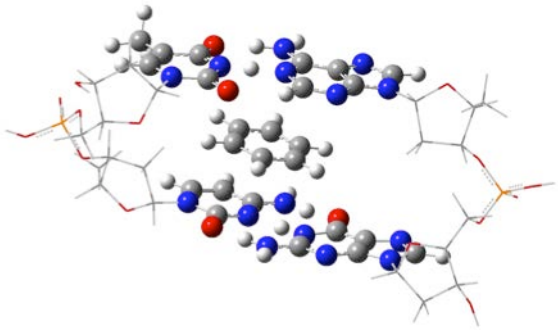

ATGC

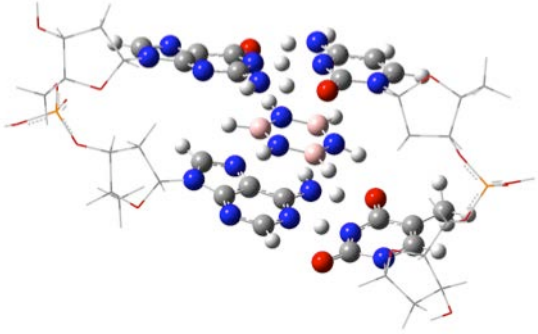

ATGCb

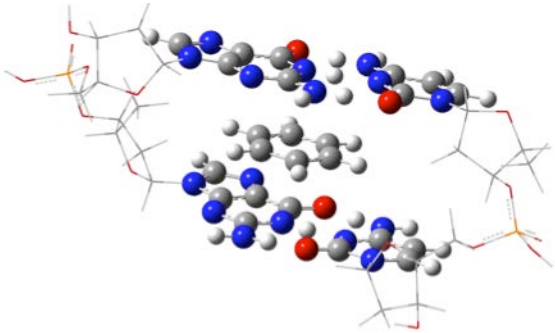

GCGC

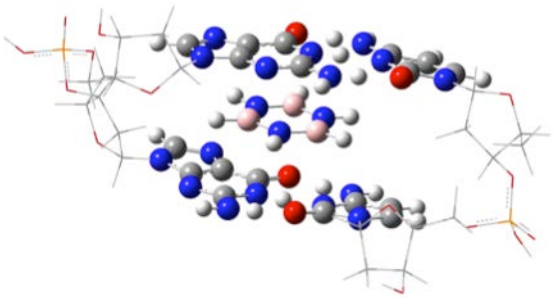

GCGCb

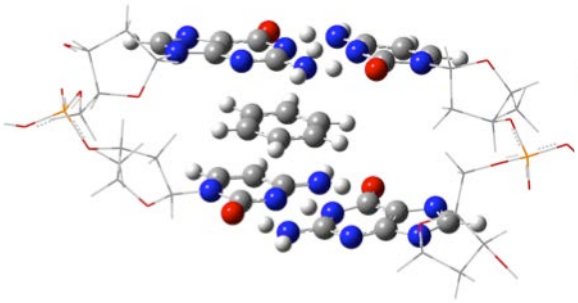

GCCG

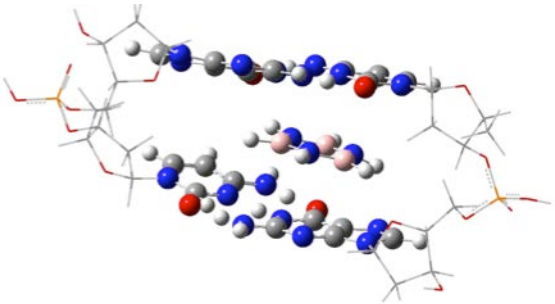

GCCGb

7.2 Charged Double-Stranded Complexes

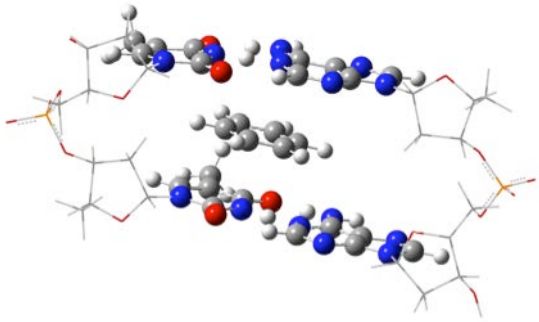

ATAT

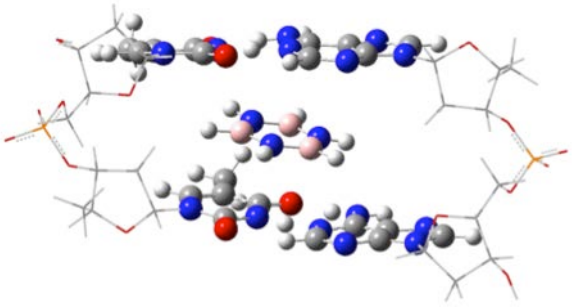

ATATb

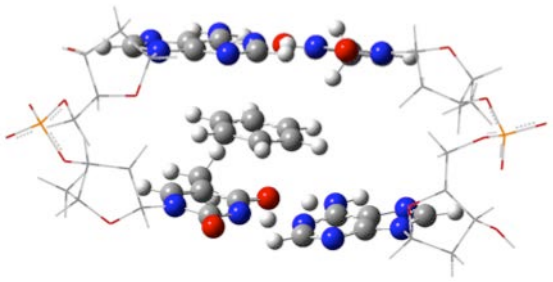

ATTA

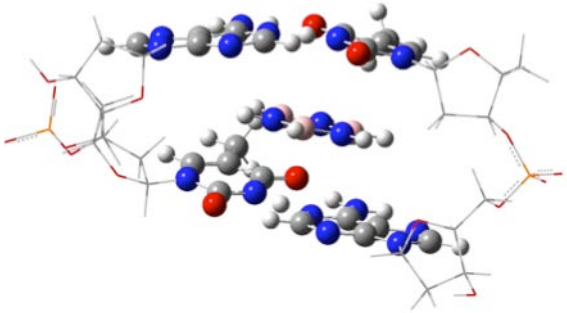

ATTAb

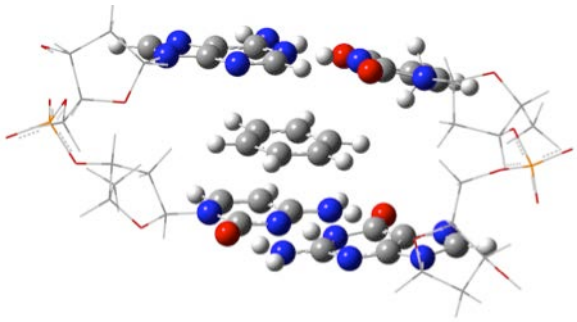

ATCG

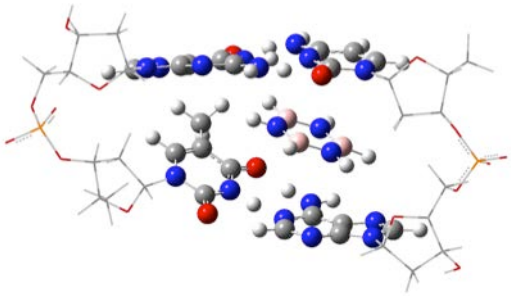

ATCGb

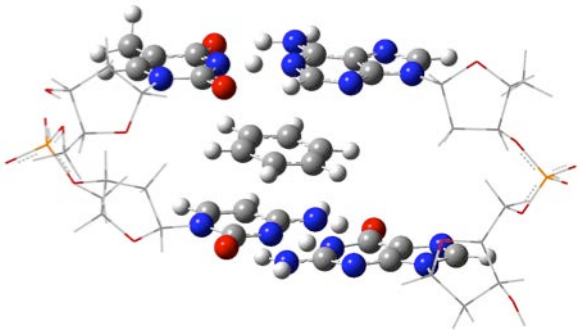

ATGC

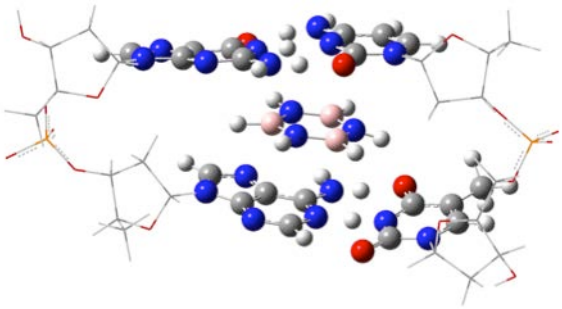

ATGCb

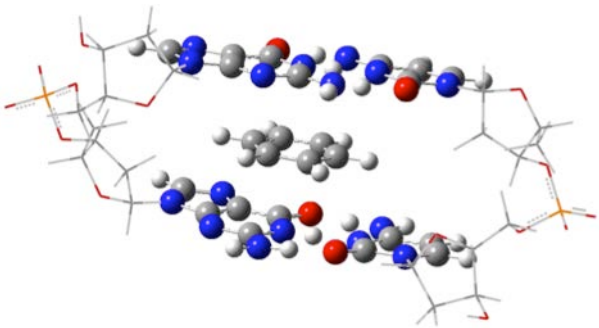

GCGC

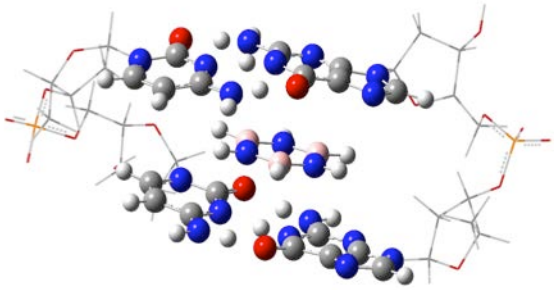

GCGCb

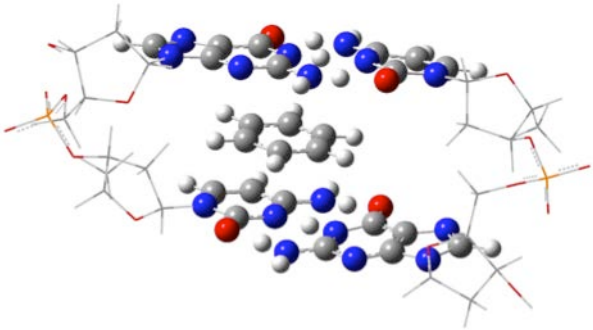

GCGC

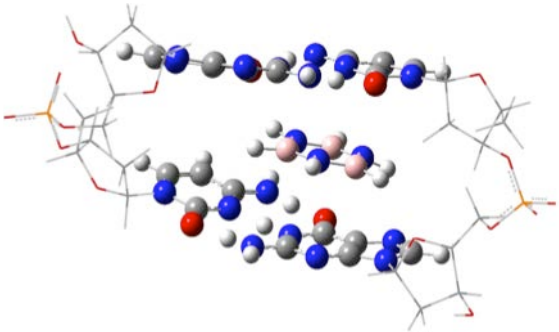

GCGCb

7.3 Charged Double-Stranded Complexes with Hybrid Intercalant

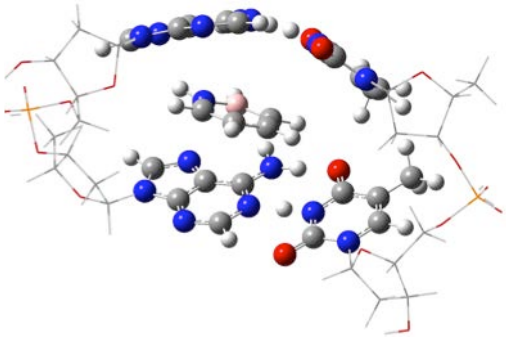

ATAT Hybrid Intercalant

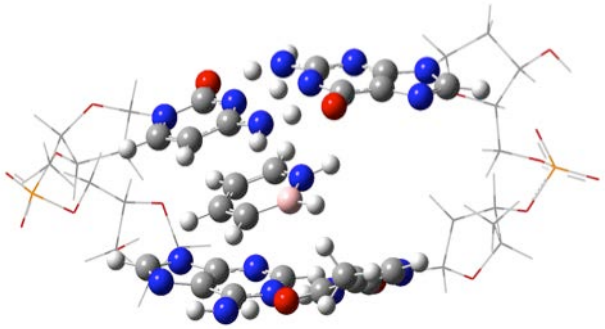

ATCG Hybrid Intercalant

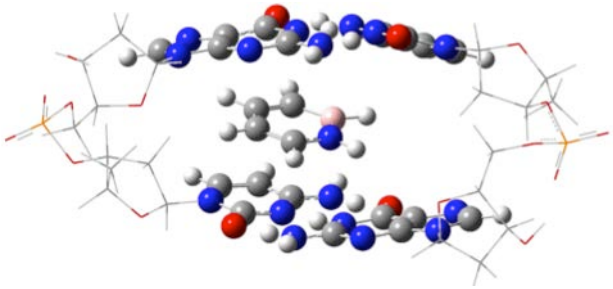

GCCG Hybrid Intercalant

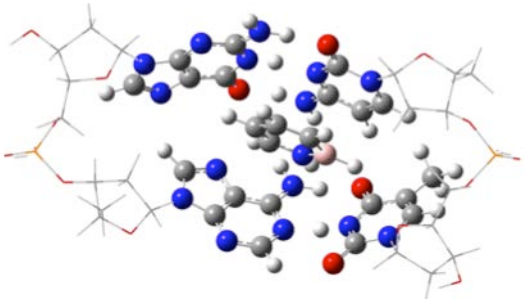

ATGC Hybrid Intercalant

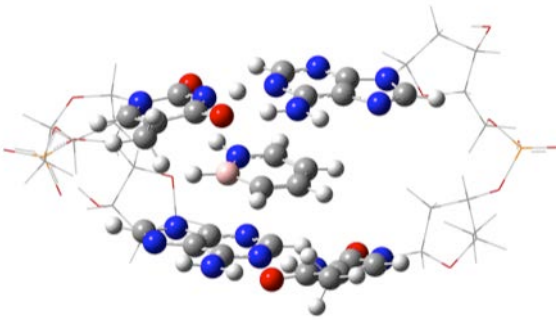

ATTA Hybrid Intercalant

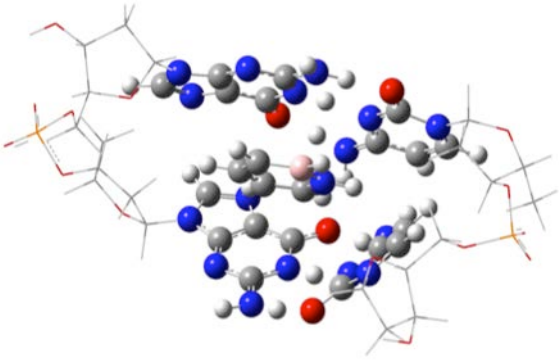

GCGC Hybrid Intercalant